I. EXECUTIVE SUMMARY

A Search for a Nonzero Strange Form Factor of the Proton at 2.5 $(\mathrm{GeV/c})^2$

A. Main physics goals

The goal for the pioneering measurement of the parity violating asymmetry (PVA) at large momentum transfer is to address the following questions:

- How large is the contribution of $s\bar{s}$ quark pairs to the hadron current at x_{Bj}=1?
- Is the lattice prediction of the almost zero values of the strange form factors consistent with an experiment?

We propose to measure the PVA for elastic electron-proton scattering by using the highly segmented NPS-type PWO-based calorimeter (ECAL) [1] as an electron arm and the segmented iron-scintillator-based calorimeter (HCAL) [2] as a proton arm in coincidence mode, using e−p angular and energy correlations for suppression of the inelastic processes.

B. The proposed measurements/observables

This experiment will detect the electron and proton in elastic electron-proton scattering. Longitudinal polarization of the electron beam will be flipped to measure the PVA. The beam polarization will be found using Compton and Moller polarimeters. The observed variable is the PVA, which is expected to be about 90 ppm. With a total of 35 days of data taking, the projected accuracy for the PVA is on the level of 5 ppm.

C. Specific requirements on detectors, targets, and beam

The experiment uses detector packages based on the NPS and HCAL components at a luminosity of 1.6×10^{38} $\mathrm{Hz/cm^2}$. The experiment will use 60 μA of a 6.6 GeV energy polarized CEBAF electron beam and a 10-cm-long LH2 target.

D. Resubmissions

The concept of this proposal overlaps significantly with PR-06-004 to PAC29. We briefly address the issues identified in the PAC29 report in the Appendix.

(A proposal to Jefferson Lab PAC50)

A Search for a Nonzero Strange Form Factor of the Proton at 2.5 $(\mathrm{GeV/c})^2$

R. Beminiwattha (spokesperson) S. P. Wells, N. Simicevic
Louisiana Tech University, LA 71272

C. Palatchi (spokesperson)
Indiana University, Bloomington, IN 47405

K. Paschke (spokesperson), S. Ali, X. Bai, G. Cates, R. Lindgren, N. Liyanage, V. Nelyubin, X. Zheng
University of Virginia, Charlottesville, VA 232904

B. Wojtsekhowski (spokesperson-contact), S. Barcus, A. Camsonne, R. Carlini, S. Covrig Dusa, P. Degtiarenko, D. Gaskell, O. Hansen, D. Higinbotham, D. Flay, D. Jones, M. Jones, C. Keppel, D. Meekins, R. Michaels, B. Reydo, G. Smith, H. Szumila-Vance, A.S. Tadepalli
Thomas Jefferson National Accelerator Facility, Newport News, VA 23606

T. Horn
Catholic University of America, Washington, DC 20064

E. Cisbani
Istituto Nazionale di Fisica Nucleare - Sezione di Roma, P.le Aldo Moro, 2 - 00185 Roma, Italy

E. King, J. Napolitano
Temple University, Philadelphia, PA 19122

P.M. King
Ohio University, Athens, OH 45701

P.A. Souder
Syracuse University, Syracuse, NY 13244

D. Hamilton, O. Jevons, R. Montgomery
SUPA School of Physics and Astronomy, University of Glasgow, Glasgow G12 8QQ, UK

P. Markowitz
Florida International University, Miami, FL 33199

E. Brash, P. Monaghan
Christopher Newport University, Newport News, VA 23606

T. Hobbs
Fermi National Accelerator Laboratory, Batavia, IL 60510

G. Miller
University of Washington, Seattle, Washington 98195-1560

J. Lichtenstadt, T. Kolar, E. Piasetzky
Tel Aviv University, Israel

G. Ron
The Hebrew University of Jerusalem, Israel

T. Averett
College of William and Mary, Williamsburg, VA 23185

S. Mayilyan, H. Mkrtchyan, A. Mkrtchyan, A. Shahinyan, V. Tadevosyan, H. Voskanyan
AANL, 2 Alikhanian Brothers Street, 0036, Yerevan, Armenia

W. Tireman
Northern Michigan University, Marquette, Michigan 49855, US

P. Datta, E. Fuchey, A. J. R. Puckett, S. Seeds
University of Connecticut, Storrs, Connecticut, 06269, USA

C. Muñoz Camacho
Université Paris-Saclay, CNRS/IN2P3, IJCLab, 91405 Orsay, France

and the NPS collaboration

(Dated: May 16, 2022)

We propose an experiment to measure the parity-violating asymmetry (PVA) in elastic longitudinally polarized beam electron-proton scattering at the momentum transfer of 2.5 $(\mathrm{GeV}/c)^2$. This experiment has the potential to discover of a non-zero strange form factor due to much higher momentum transfer than was previously investigated and several times higher relative precision of measuring the PVA.

The proposed measurement of PVA will allow us find or put an upper limit on the strangeness form factor, specifically a combination $\epsilon G_E^s + \tau G_M^s$ at $\epsilon = 0.94$ and $\tau = 0.71$. The projected statistical uncertainty of the PVA is 5.8%, which could be translated to the ratio of SFF to the Dipole fit of the nucleon form factor of 5.0%. The result will be used in flavor decomposition of the nucleon form factors.

The time coincidence between the scattered electrons and recoil protons detected in the shower counters will be used for the identification of the elastic process. The angular and energy correlations will be measured accurately.

In 35 days of beam time at 6.6 GeV and a 60 μA beam with 80% polarization on 10-cm-long liquid hydrogen target, the parity-violating asymmetry PVA will be measured to a statistical precision of ± 5 ppm. This measurement will present an important development in the experimental study of the $s\bar{s}$ content of the nucleon, nucleon form factor flavour decomposition. The structure of the detector setup allows future extensions of this measurement to the quasi-elastic processes on deuterium and a Rosenbluth separation of the G_E^s and G_M^s, which requires much more beam time.

CONTENTS

II. INTRODUCTION

The investigation of strange form factors (SFF) is one of the most active research fields: see reviews [3, 4]. There are several reasons which justify serious present and future experimental efforts to study SFF. First of all, SFF were never measured before at momentum transfer above 1 $(\mathrm{GeV}/c)^2$, so the observation and potential discovery of non-zero SFF properties will be very important for the deeper understanding of the nucleon structure, and it will provide essential input for the development of theory. Other motivations include testing of the links between SFF and the results from the polarized DIS lepton and neutrino scattering and testing of the predictions of the effective theory of SFF. Polarized elastic electron scattering on the proton, suggested for measurement of the $s\bar{s}$ content [5–7], has been realized in several experiments [8–11]. In addition, flavor decomposition of the nucleon form factor [12], which allows us to advance our understanding of the G_E^p/G_M^p reduction discovered at JLab with an increase of momentum transfer [13], requires experimental data on SFF.

SFF have been found consistent with zero at low momentum transfer and could be explained by several effects, see e.g. review [14]. The variation of SFF with momentum transfer Q^2 is a subject of great interest. One possible hypothesis is that SFFs have a Q^2 dependence similar to that of the G_E^n form factor but at higher Q^2 due to a much larger strange quark mass.

Presently used experimental techniques in studies of PVA in elastic e−p scattering are based on two approaches. The first one is the integration method, used at SLAC in a pioneering experiment [15], and further developed at MIT-Bates in a ^{12}C experiment [8] and at Mainz in a Be experiment [16]. Two recent experiments based on the integration method are SAMPLE [17, 18] and HAPPEX [9, 19, 20]. The second method is based on counting of the events for different helicities of the electron beam. Two experiments based on the counting method are G0 [10] and A4 [11]. The apparatus of G0 has two configurations for detecting only the recoil protons or only the scattered electrons.

At low Q^2 both methods achieved very high accuracy; however, measurements at Q^2 larger than 0.8 $(\mathrm{GeV}/c)^2$ become less accurate due to growing background and/or statistical uncertainties [10]. **We are proposing to use a counting method in coincidence mode**. A scattered electron and a recoil proton will be detected with a time resolution of a few nanoseconds, tight angular correlations, and effective rejection of the low energy background. Such a technique will allow us to use non-magnetic detectors for both the electron and the proton, cover the full solid angle possible for given Q^2 and operate at high luminosity. The proposed approach is based on the segmented calorimeter which was used in our previous experiments at JLab at similar beam energy and luminosity. The proposed configuration has an effective electron solid angle near 42 msr which is about 8 times larger than the solid angle of a universal magnetic spectrometer such as HRS.

We therefore propose a measurement of PVA asymmetry in elastic e−p scattering at an incident energy of 6.6 GeV and average scattering angle of 15.5°.

The text of the proposal is organized as follows. In Section III we describe in some detail the formalism of PVA asymmetry and the possible values for SFF. In Section IV we describe the experimental approach. In subsequent sections, we present the proposed measurements (Sec. V), the expected results and beam time request (Sec. VI), and the technical considerations related to the equipment (Sec. VII). The proposal concludes with a Section VIII. Appendix, which has the PAC29 report on the original proposal PR-06-004 and addresses the issues identified in the PAC29 report.

III. PHYSICS MOTIVATION

A. Overview

There are several interesting questions that motivate us to explore the measurement of PVA in e−p elastic scattering at large Q^2:

1. Are SFF non-zero at large Q^2?
2. What is the Q^2 dependence of the strange form factors?
3. What are the constraints on the proton 3D image imposed by the proposed measurement of the $s\bar{s}$ content?
4. How will SFF impact flavor decomposition of the nucleon FF?

We will discuss to what level of accuracy SFF could be measured at the proposed and other kinematics.

B. PVA asymmetry

The effect of lepton helicity in photon-hadron reactions was first considered by Zel'dovich [21], who estimated the size of the PVA asymmetry. PVA in electron scattering has become an effect of large interest since the development of the Standard Model. Investigation of the spin sum rule in DIS led to a huge jump in interest in the role of the strange quarks in the nucleon structure. An experimental approach was proposed by McKeown [6] and Beck [7], who demonstrated how to measure SFF by using elastic electron-proton scattering.

The asymmetry A_{PV} in e−p elastic scattering can be expressed as:

$$A_{PV} = -\frac{G_F Q^2}{4\pi\alpha\sqrt{2}} \cdot [(1 - 4\sin^2\theta_W) - \frac{\epsilon G_E^p G_E^n + \tau G_M^p G_M^n}{\epsilon (G_E^p)^2 + \tau (G_M^p)^2} - \frac{\epsilon G_E^p G_E^s + \tau G_M^p G_M^s}{\epsilon (G_E^p)^2 + \tau (G_M^p)^2} + \epsilon'(1 - 4\sin^2\theta_W)\frac{G_M^p G_A^{Zp}}{\epsilon (G_E^p)^2 + \tau (G_M^p)^2}] \quad (1)$$

where $G_F = 1.17 \cdot 10^{-5}$ GeV^{-2} is the Fermi coupling constant and $G_{E(M)}^{p(n)}$ are the electric (magnetic) Sachs form factors of the proton (neutron), θ_W is the weak-mixing angle, $\sin^2\theta_W = 0.2312$, G_A^{Zp} is the neutral weak axial form factor of the proton, and τ, ϵ, and ϵ' are kinematic parameters:

$$\tau = \frac{Q^2}{4M_p^2},\ \epsilon = \left[1 + 2(1+\tau)\tan^2(\theta/2)\right]^{-1},\ and\ \epsilon' = \sqrt{\tau(1+\tau)(1-\epsilon^2)} \quad (2)$$

The values of four terms in parenthesis in the Eq. 1 are: 0.0752; 0.6103; 0; and 0.1707. Here the $G_{E(M)}^s$ are assumed to be zero.

The value of A_{PV} is the subject of electroweak radiative corrections which are considered in a number of papers, see e.g. Refs. [14, 22].

C. Expected accuracy for the parity valuation asymmetry

Assuming 5 ppm statistical accuracy for the experimental raw asymmetry (total statistics of 4×10^{10} elastic e−p events) we can evaluate the precision for SFF (see calculation of statistics in section V).

Let us evaluate the components of expression 1 at the kinematics of this proposal. At the proposed forward scattering kinematics $\epsilon = 0.94$, $\tau = 0.71$, $\epsilon' = 0.38$, and $\epsilon'(1 - 4\sin^2\theta_W) = 0.041$. PVA is sensitive to the combination of strange form factors which could be approximated by $\epsilon(G_E^s + \tau\,\eta\,G_M^s)/G_D$ with $\eta = G_M^p/\epsilon G_E^p \sim 0.24$ at Q^2=2.5 $(\mathrm{GeV}/c)^2$. To make such an estimate we assumed the approximation (except for η) that G_M^p, G_M^n form factors are equal to the charge $(\mu) \cdot G_D$ and G_E^n, follows the Galster fit.

Information on G_A^{Zp} at large momentum transfer becomes sufficiently accurate, thanks to the studies in the Dyson-Schwinger approach [23, 24] (see Fig. 1) , development of the GMDs models [25], and the results from lattice calculation [26]. The remaining uncertainties in G_A^{Zp} due to higher order corrections are currently a subject of active research. The G_A^{Zp} fit relative uncertainty at

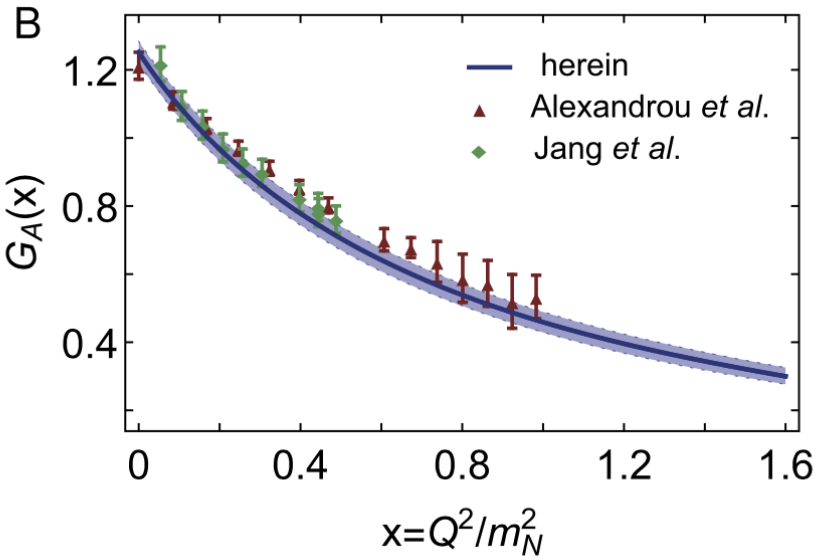

FIG. 1. The axial form factor results from Ref. [23].

2.5 $(\mathrm{GeV}/c)^2$ is about 3.6% with $g_A = 1.25(3)$ and a mass-scale $M_A = 1.23(3)\,m_N$ [23, 24]. The G_E^n is currently known at Q^2 range 1-3 $(\mathrm{GeV}/c)^2$ to 10% relative accuracy [25, 27] which contributes 1% to the uncertainty of PVA.

The measurement of PVA with a relative accuracy of 5% will lead to a determination of $(G_E^s + \eta G_M^s)/G_D$ to an accuracy of 0.0025 or alternatively to a level of 5% of G_D. From such an estimate we can see that a measurement of PVA to a relative accuracy of 5% is consistent with the accuracy of measurements for other parameters which contribute to PVA.

D. Counting rate vs. momentum transfer

The measurement of PVA requires a large solid angle for the detector. Let us present the cross section as a function of Q^2:

$$\frac{d\sigma}{dQ^2} = \frac{4\pi \cdot \alpha^2}{Q^4} \cdot \left(1 - \frac{Q^2}{2EE'}\right) \frac{E'}{E} \cdot |F^2| \tag{3}$$

$$|F^2| = |G_E^p(Q^2)|^2 \left[\frac{(2 - \frac{Q^2}{2ME})^2}{1+\tau} - \frac{Q^2}{E^2}\right] + \tau |G_M^p(Q^2)|^2 \left[\frac{(2 - \frac{Q^2}{2ME})^2}{1+\tau} + \frac{Q^2}{E^2}\right]$$

At the proposed kinematics where $\tau \sim 0.71$ we can neglect Q^2/E^2, which is just 1/18. The average value of Q^2 over the experimental acceptance is dominated by the low Q^2 side just because of the fast fall of the form factors with Q^2, so we have to deal with a very simple expression:

$$\frac{d\sigma}{dQ^2} \approx \frac{4\pi \cdot \alpha^2}{Q^4} \cdot \frac{1 + \tau\mu^2}{(1 + Q^2/0.71)^4} \frac{1 - 2\tau M/E}{1+\tau} \tag{4}$$

At a given Q^2 it is useful to select a range of $\Delta Q^2/Q^2 \approx 0.2$, where the rate variation isn't too large. The exact range of ΔQ^2 will be defined during the design of the apparatus based on considerations, such as background rate and detector cost. At the same time, a complete 2π azimuthal coverage is desirable.

E. Precision vs. momentum transfer

The proposed setup could be used for A_{PV} measurement at several values of Q^2. Figure 2 shows the differential cross section $d\sigma/dQ^2$, the integrated cross section in the detector acceptance $d\sigma/dQ^2 \cdot 0.2 \cdot Q^2$, and a Figure-of-Merit (FOM) $d\sigma/dQ^2 \cdot 0.2 \cdot Q^2 \cdot A_{PV}^2$ vs. the momentum transfer. The drop of the FOM with Q^2 is slow ($\propto 1/Q^2$), so the accuracy of the measurement is still quite

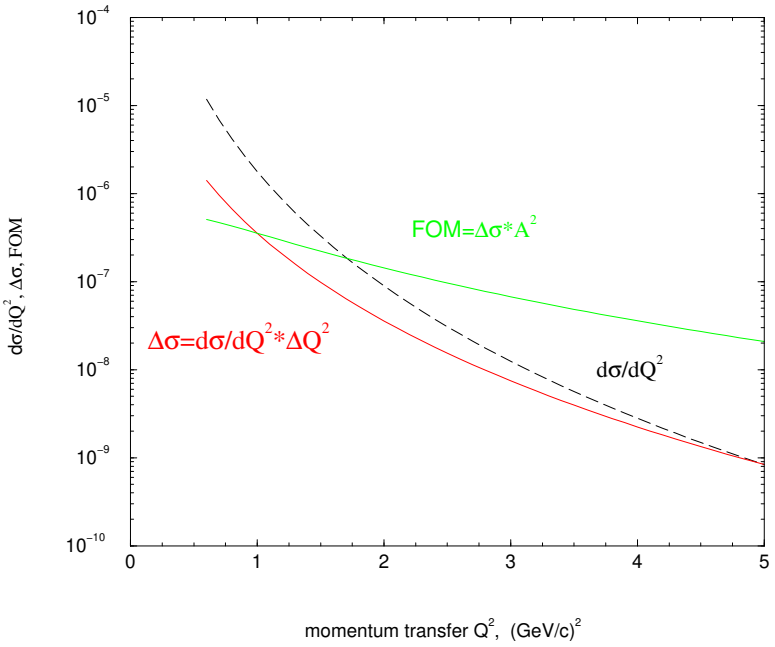

FIG. 2. The differential cross section of e−p elastic scattering at beam energy 6.6 GeV - $d\sigma/dQ^2$, integrated cross section in the detector acceptance $0.2 \cdot Q^2$, and a Figure-of-Merit $d\sigma/dQ^2 \cdot 0.2 \cdot Q^2 \cdot A_{PV}^2$ as a function of Q^2.

good, even at 3 $(\mathrm{GeV}/c)^2$. The size of the detector apparatus and the background rates for the proposed kinematics will be discussed in section IV.

F. Form factors in the GPD approach

A GPD formalism recently developed for the description of the exclusive electromagnetic processes provides a framework for the interpretation of many observables [25, 28, 29]. Form factors of

the nucleon are presented as

$$F_1(t) = \sum_{a=q,\bar{q}} e_a \int_{-1}^{1} dx\, H^a(x,0,t),$$
$$F_2(t) = \sum_{a=q,\bar{q}} e_a \int_{-1}^{1} dx\, E^a(x,0,t).$$

The connection to DIS gives information about GPDs in the limit $t = 0$.

$$H^a(x,0,0) = q^a(x),$$
$$\hat{H}^a(x,0,0) = \Delta q^a(x).$$

The function E^a allows the total angular moment of a quark of flavor a to be determined through Ji's sum rule.

$$E^a(x,0,0) = 2\frac{J^a(x)}{x} - q^a(x),$$

The recent models for GPDs were developed in [25]. They factorize GPDs as a product of a quark distribution $q(x)$, measured in DIS, and an additional function of x and t.

$$H_v^q(x,t) = q_v(x)\, \exp\left[t f_q(x)\right]$$

$$q_u^{val}(x) = 1.89\, x^{-0.4}\, (1-x)^{3.5}(1+6x)$$

$$q_d^{val}(x) = 0.54\, x^{-0.6}\, (1-x)^{4.2}(1+8x)$$

where the functions $f_q(x)$ were parametrized and fit to describe the form factors $F_1(t)$ and $F_2(t)$ for the proton and the neutron. The fits for SFF obtained in Ref. [25] are shown in Fig. 3. Interpolation

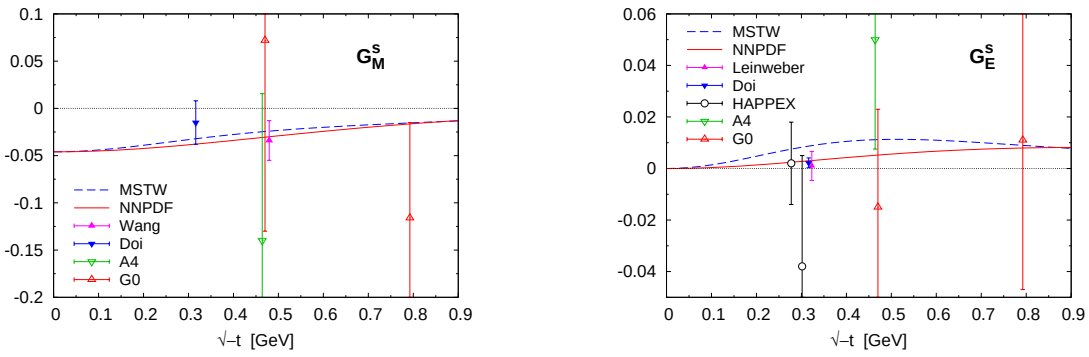

FIG. 3. The fit of strange form factors vs. momentum transfer per Ref. [25].

on this plot for G_E^s to Q^2=2.5 $(\mathrm{GeV}/c)^2$ provides a value of 0.01.

G. World data for SFF

The main trend of Q^2 dependence for the electromagnetic form factors at Q^2 below 3 $(\mathrm{GeV}/c)^2$ is described by the dipole formula. From the large mass of the strange quark one can expect that the Q^2 dependence of the SFF is slower compared to the light quark part of the form factors. Because SFF are related to the Z-boson exchange, the probe has a very small size, and the Q^2 dependence in the range below 1 $(\mathrm{GeV}/c)^2$ should be much slower than for electromagnetic form factors, which means that the size of SFFs relative to the electromagnetic form factors is growing [30]. In DIS neutrino at $Q^2 = 16$ $(\mathrm{GeV}/c)^2$ the observed contribution of $s\bar{s}$ is above 50% [31], which may indicate that in elastic electron scattering at large Q^2 the relative size of SFF could also be large. Finally, published G0 data shown in Fig.4, indicate a possible rise of SFF with Q^2 [10], which must be investigated by measurement of A_{PV} at larger momentum transfer.

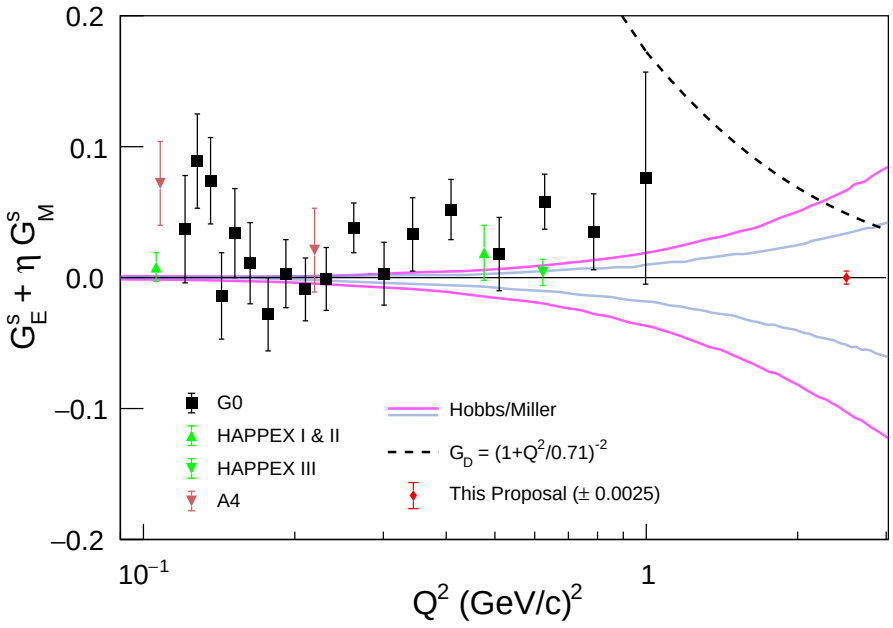

FIG. 4. The strange form factor vs. Q^2 according to the G0 experiment [10], HAPPEX, A4 and expected accuracy of this proposal. The blue and pink lines show the area of acceptable value of SFF according to analysis [32, 33].

The Q^2 dependence of G_E^n reflects two competing effects, each of which has its own momentum scale. The scale of G_E^n rise is due to separation between light quarks. This effect is also present in SFF; however, the scale could be shorter or longer, depending on the dominant mechanism. The fall is due to the nucleon wave function defined by quark-gluon interaction and interpolated by dipole fit. The fall of SFF most likely has a similar origin; however, it may have a different scale of Q^2. Figure 4 shows the world data and expected accuracy of the proposed measurements.

Figure 4 also shows the result of the recent analysis performed by T. Hobbs, M. Alberg, and G. J. Miller on the possible size of the SFF [32, 33], according to which even the value of SFF on the level of G_D is not excluded.

IV. EXPERIMENTAL SETUP

The proposed experiment will study scattering of polarized electrons from a liquid hydrogen target, as illustrated in Fig. 5. The key considerations of the experimental approach are presented

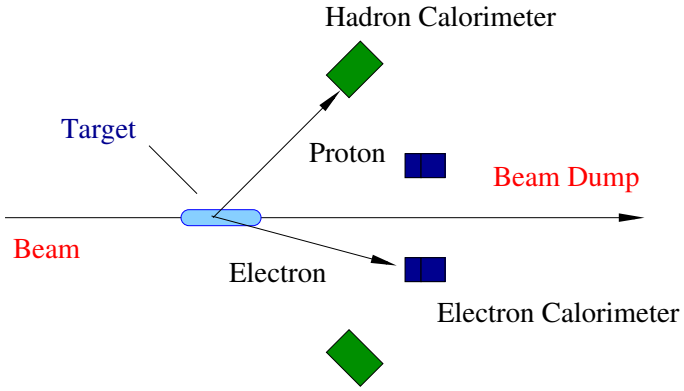

FIG. 5. Schematic of the experimental setup. The target is a liquid hydrogen 10-cm-long cylinder. Scattered electrons are detected in the inner ring (electromagnetic calorimeter) and recoil protons are detected in the outer ring (hadron calorimeter).

here:

- Elastically scattered electrons have the maximum kinetic energy among all particles at any given scattering angle.
- Amplitude spectra from an electromagnetic shower calorimeter drop very fast, so at the top of the spectra, elastically scattered electrons contribute a large portion to the detector rate even at a few $(\mathrm{GeV}/c)^2$ momentum transfer.
- Recoil protons of 1 GeV kinetic energy will be detected with high efficiency by a hadron shower calorimeter even with a relatively large threshold.
- The counting rate at a few $(\mathrm{GeV}/c)^2$ is sufficiently low for use of the coincidence technique with a segmented detector system.
- Coincidence between the signals from an electron and a proton detector and perfect kinematical correlation in azimuthal and polar angles of an elastically scattered electron and a recoil proton allow for clean events of elastic scattering with a simple non-magnetic detector system.
- A non-magnetic detector system based on shower calorimeters allows us to cover the largest solid angle useful for a given Q^2, which is selected based on variation of the counting rate with the scattering angle.
- A large value of A_{PV} allows a precision measurement of SFF at 2.5 $(\mathrm{GeV}/c)^2$ within a moderate beam time of one month.

A. Overview

Scattered electrons will be detected in a segmented electromagnetic calorimeter installed at an average polar angle of $15.5\pm1^\circ$, and recoiling protons will be detected in the segmented hadron calorimeter at a polar angle of $42.5\pm2^\circ$. Due to the significant length of the target, reconstruction

using only the electron arm is not ideal for elastic event selection. Reconstruction will be achieved by a combination of data from both arms. The natural coordinate resolution of the hadron arm of 7 cm will be improved by a pre-shower layer: an array of small plastic scintillator counters behind a 3" thick lead wall. These counters will provide a proton coordinate with an accuracy of 0.5 cm.

In off-line analysis the electron polar angle will be reconstructed with an accuracy of 0.18° defined by the length of the target. The proton polar angle will be reconstructed off-line with an accuracy of 0.32°, which dominates from contribution of the target length.

More specific geometry of the detector and the DAQ considerations presented here are based on the round shape of the configuration which simplifies discussion of the concept of overlaps. However, it will require adjustment due to the rectangular shape of the individual counters, which we omitted on the current level of design. A possible geometry implementation is shown in Fig. 6.

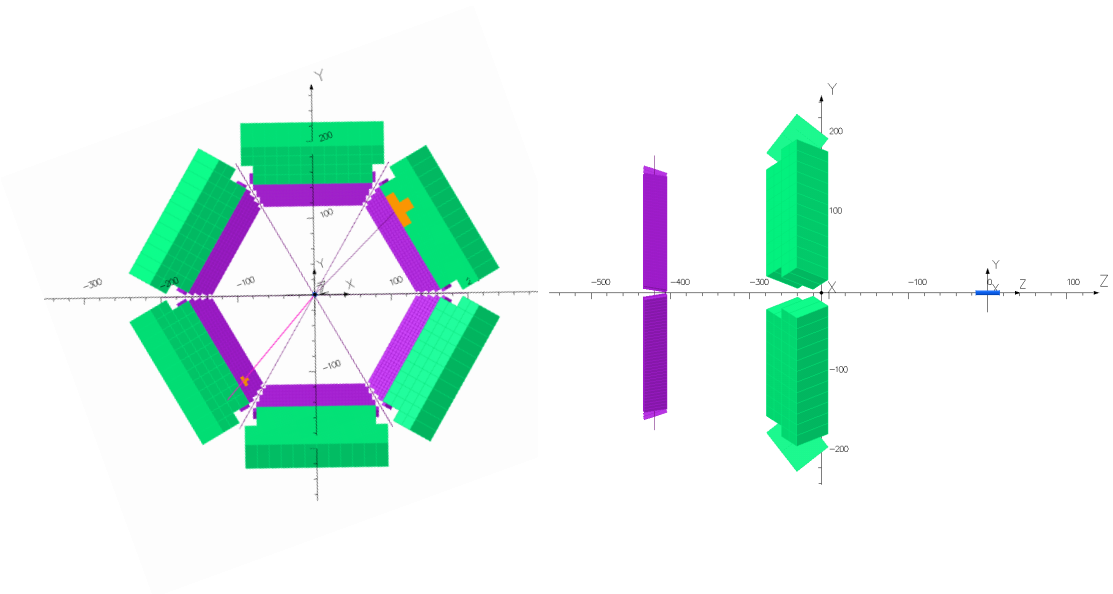

FIG. 6. The option for detailed geometry of the detector.

Radiation dose

The estimate for total energy deposition in the detectors was calculated by using MC results presented in Fig. 7. Contribution of secondary electrons is dominant in the energy flow. The total dose in the ECAL crystal (beyond first 2 cm of depth) over duration of data taking (2.6×10^6 sec) was found to be less than 34 kRad, which leads to reduction of the signal by 2% [34]. This estimate used 28 MeV cut off energy. The LED based annealing system is already implemented in the NPS calorimeter and will be used as needed. If 10 MeV is selected as energy cut-off for dose analysis, the result is 10 times higher but it is still low enough when daily radiation annealing is used.

Signal pileup and energy resolution

The same information on the energy flow allows us to make an estimate of the base line shift and fluctuation. The total energy flow in one crystal of ECAL during a 40 ns time window is 28 MeV. The dominant contribution to energy flow is due to electrons with energy above 30 MeV. The electrons with energy below 30 MeV will effectively stop in the first 2 cm of the crystal and produce

less light. The upper limit for the fluctuation corresponds to 20 MeV or 0.4% of the full energy of the elastically scattered electron.

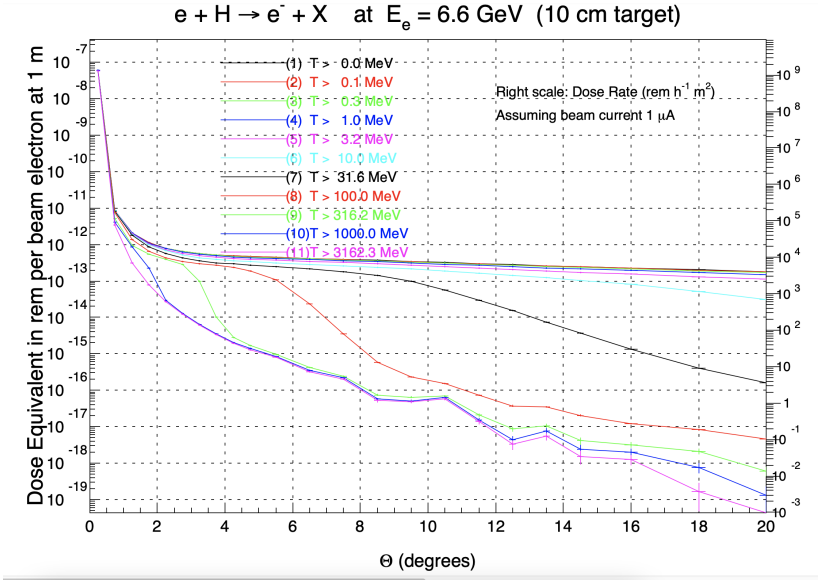

FIG. 7. The electron energy flow for 6.6 GeV electron beam on 10-cm-long LH2 target [35].

B. Electron arm structure

A total of 1000 PWO crystals will be used in the electron arm. They are arranged with five at a given azimuthal angle. Such a group size includes one crystal on each side for high energy resolution when an electron hits the inner portion, effectively 1.7 crystals for the required polar angle range of 1.44 degree, and 1.3 degree due to the 10-cm-long target viewed at a 15.5 degree polar angle. There are a total of 200 groups of 5 at the different azimuthal angles. Each detector covers an azimuthal angle of 1.8°. Each electron detector has face dimensions 2x2 cm^2 at a distance from the target of 239 cm. The range of polar scattering angles of the electrons with high energy resolution is defined by a full angular coverage of the detectors of 1.44°, which corresponds to $\Delta Q^2/Q^2 = 0.2$. The solid angle of the electron arm with high energy resolution is 42 msr (for the central ΔQ^2 range). The coordinate resolution of the PWO calorimeter is 0.2 cm at 5 GeV. The expected energy resolution at electron energy of 5 GeV is 2.2%.

Total rate of elastic events within high resolution area for electron arm is 15 kHz after taking into account radiative tail.

For DAQ consideration in the electron arm there are 200 groups, each of them including 5 x 5 counters (25 for every azimuthal group). The azimuthal subsystems have overlaps with adjacent subsystems of two crystals on each side. The trigger of the experiment will be made as OR of 200 subsystems. For each, the threshold will be 4.5 GeV using the VME-based trigger system [36]. Each electron arm DAQ subsystem will cover 9° in the azimuthal angle (with 80% overlap) and solid angle of 1.8 msr (for the background counting rate analysis).

C. Proton arm structure

A total of 288 iron-scintillator detectors will be used in the proton arm. The individual proton detector has face dimensions 15.5 x 15.5 cm^2. The detector will be located at a distance of 351 cm from the target. Each detector covers a solid angle of 2.0 msr. Detectors will be arranged with three at the given azimuthal angle. This will provide two detectors with full resolution. These two central detectors will cover the required range of polar angles of 4.9 degrees, plus the extra 6.8 cm required due to the 10-cm-length of the target viewed at a 42.5 degree polar angle.

There are a total of 96 groups of three at different azimuthal angles. For the DAQ of the proton arm we will arrange overlapping subsystems of 3 x 3 detectors in each. There are 96 overlapping DAQ subsystems in the proton arm.

D. Trigger rates

A threshold in the electron arm trigger will be at the level of 4.5 GeV or 85% of a 5.34 GeV signal from the elastically scattered electrons. The electron trigger counting rates are dominated by the DIS event rate, which at the on-line threshold value is about 5 times above the elastic event rate. The total rate is estimated to be on the level of 136 kHz for the full electron arm (1000 counters) using cross section results presented in Fig. 8. A threshold in the proton arm trigger will be at the

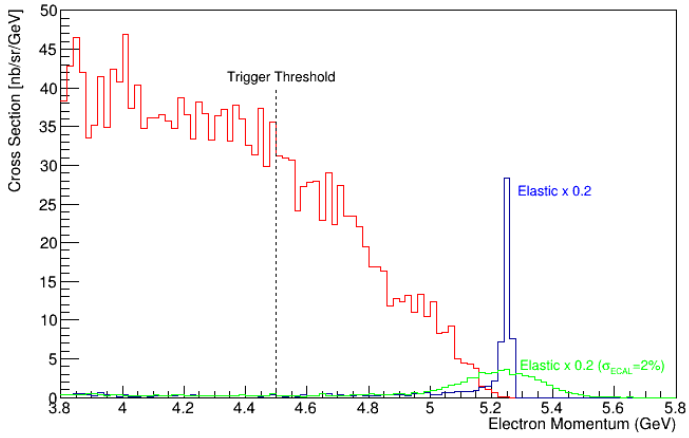

FIG. 8. The cross section of DIS e−p for 6.6 GeV initial beam energy and 15.5° scattering angle.

level of 50 MeV, which leads to 90+% detection efficiency for protons with 1.3 GeV kinetic energy. The hadron trigger counting rate is estimated to be on the level of 1.2 MHz for the full hadron arm (288 counters) using the PYTHIA-based rate results presented in Fig. 9.

E. Detailed trigger structure

Scattered electrons will be detected in a segmented electromagnetic calorimeter installed at an average polar angle of 15.5°, and recoiling protons will be detected in the segmented hadron calorimeter at a polar angle of 42.5°. About 15-17% of electrons will be in the radiative tail below 4.5 GeV. The rate of each 200-electron-arm subsystem will be 5.5 kHz inelastic and about 1.3 kHz elastic events.

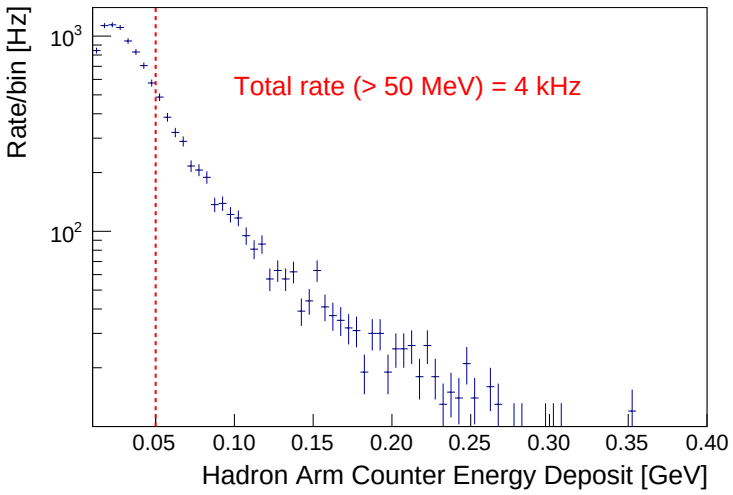

FIG. 9. The hadron rate vs. threshold for 6.6 GeV beam energy for 2 msr solid angle and 42.5° scattering angle at luminosity 1.6×10^{38} electron-nucleon per second.

A threshold in the proton arm trigger will be at the level of 50 MeV which leads to 90+% detection efficiency. The rate of each 96 proton arm subsystem will be 36 kHz.

We plan to use a 40 ns time window for coincidence in the on-line trigger logic. Each DAQ subgroup includes 25 electron and 9 proton detectors. The projected rate of coincidence of one electron subsystem and one proton subsystem has 8 Hz of accidentals and 1.3 kHz of real coincidence events.

In off-line analysis several cuts will be applied: the time window reduced to 4 ns, the coordinate in the electron arm reduced to a central portion of 3 x 1 counters, the coordinate in the proton reduced to a central portion of 2 x 1 counters. These changes lead to an accidental rate estimate of 0.02 Hz and elastic rate of 1.3 kHz. The remaining accidental background will be reduced by an additional factor of 10 by removal of events with electron energy below 5.223 GeV.

At this level of analysis the real coincidence contains mostly elastic events, thanks to good energy resolution of the PWO calorimeter. The accidental events rate is mainly due to the elastic electrons coinciding in time with unrelated protons. Most of those events will be removed by a tight cut on angular correlation (two-sigma): missing proton perpendicular momenta limited from the coordinate resolutions, so product is of $4\pi * 0.2 * 0.8 \times 4\pi * 1.32 * 1.36$, which is much smaller than the average for the area of detectors - $2 * 15.5 * 15.5 \times 3 * 2 * 2$. A corresponding reduction factor is of 13. This will bring the Real/Accidental ratio to the level of 0.8×10^7.

Some of accidental protons are from hyperon photo-production and could have PV asymmetry. A further discussion of this contamination will be presented in section V D.

F. The CEBAF polarized electron beam

We assume an incident electron beam intensity of 60 μA with 80% polarization. Such currents and polarizations have already been delivered using the strained GaAs source at Jefferson Lab. Compton and Moller polarimeters will be used to monitor the beam polarization. A system of BPMs and BCMs developed by the JLab parity collaboration will be used to ensure parity-quality beam. A raster of the beam will be used to reduce heat density in the target and increase the boiling limit. A system of small angle Lumi counters will be used to monitor the level of target boiling

noise.

G. The hydrogen target and the radiator

In this experiment we will use the standard Hall C liquid hydrogen target with a 10-cm-long target cell to provide an almost 360° azimuthal aperture for detection of the particles in the forward direction from 14.5 to 45°.

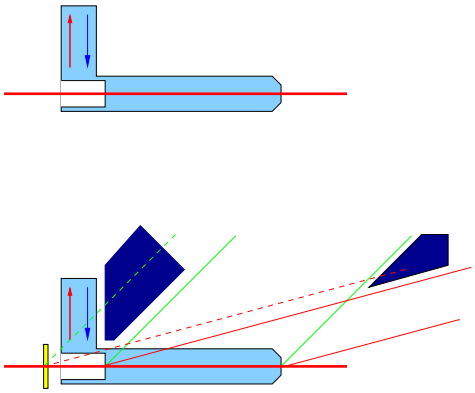

FIG. 10. Side view of the liquid hydrogen target with a radiator and a collimator on the second loop. The green lines show the aperture of the proton detector. The red lines show the aperture of the electron detector. A red dotted line shows the electron scattered in the radiator at 15.5° to the electron detector and absorbed in the shielding block.

The scattering chamber with suitable geometry is shown in Fig. 11. It was used in DVCS experiment [37]. This scattering chamber allows the large diameter exit pipe essential for low background operation.

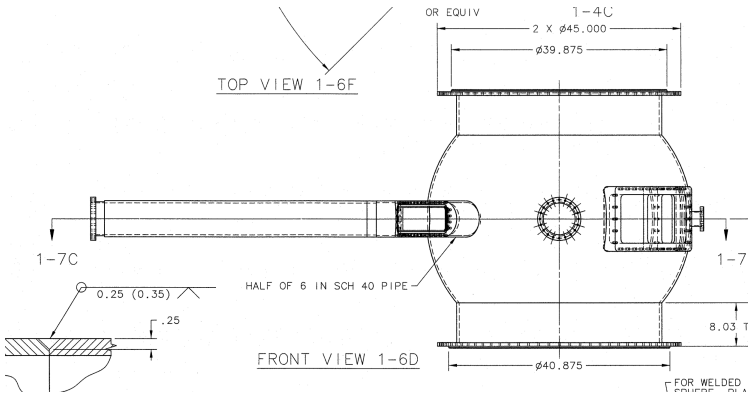

FIG. 11. Side view of the semi-spherical scattering chamber used in DVCS experiment.

A measurement of the single pion production background will be done with the help of a radiator in front of the second loop of the target system. The radiator will be mounted on a liquid helium block about 40 cm upstream of the target center. The short distance between the target and radiator helps avoid background produced from the Al walls of the target and the downstream beam line. At the same time, the distance is sufficient to arrange shielding which blocks the protons and electrons produced by the radiator from reaching the detectors.

H. The electron calorimeter

The proposed ring electromagnetic calorimeter (EMC) has a radius of 64 cm and consists of 1000 blocks with face dimensions of 2x2 cm^2. The EMC will be constructed from components of the NPS calorimeter [1]. Such an option will provide superior 2.2% energy resolution for 5.34 GeV scattered electrons and 0.2 cm coordinate resolution. Energy and time resolution are the primary parameters needed for the EMC. An intrinsic time resolution of 1 ns will allow a 40 ns time window on-line and just 4 ns for off-line analysis. Figure 12 shows the side view of the calorimeter.

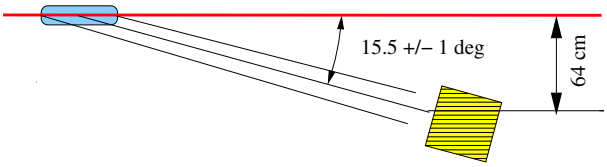

FIG. 12. The structure of the electron detector - a ring calorimeter.

I. The hadron calorimeter

The proposed ring hadron calorimeter (HCAL) has a radius of 237 cm and consists of 288 blocks with face dimensions of 15.5x15.5 cm^2. A simple option for the HCAL is iron-plastic plates sandwiched with wave-shifter light collection. Such an option will provide about 30-40% energy resolution for 1 GeV kinetic energy of the recoil proton. The hadron calorimeter components of the SBS spectrometer could be re-used after completion of the SBS program in Hall A. Figure 13 shows the concept of the proton detector.

An additional detector of the hadron arm is the highly segmented scintillator hodoscope. Each counter of this array is 2 x 2 x 10 cm with wave-length shifting fiber for readout by a 64-pixel PMT. It will be protected from the target by a 3 inch wall of lead. Such counters will detect the initial proton with a coordinate accuracy of 0.5 cm. The total number of channels in the scintillator array is 45700, which will require about 700 64-pixel PMTs.

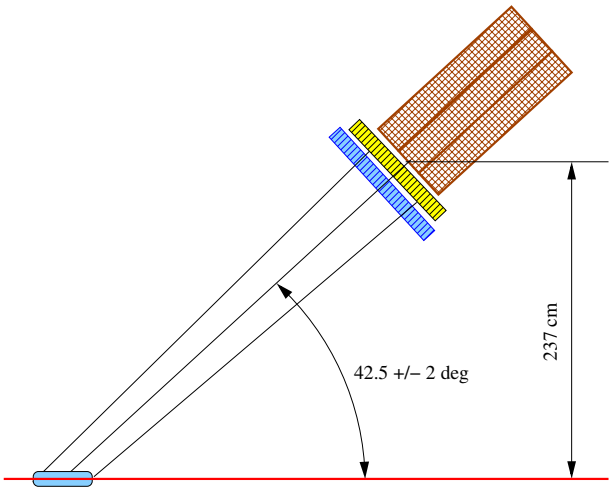

FIG. 13. The structure of the proton detector: a ring array of iron-plastic counters is shown in red; an array of small scintillators shown in yellow; a 3 inch lead wall is shown in blue.

V. PROPOSED MEASUREMENTS

A longitudinally polarized electron beam with a current of 60 μA at an energy of 6.6 GeV will be used with a 10-cm-long target of liquid hydrogen. A Cu radiator with a thickness of 0.8 mm (6% radiation length) will be installed 8 inches upstream of the target on the second loop used for background study. The recoil proton will be detected in the hadron calorimeter with an array of small scintillators for better coordinate measurement. The scattered electron will be detected in the electromagnetic calorimeter. All features of the experimental technique have been used before at Jefferson Lab or are well developed.

A. The kinematics and counting rate

The average momentum of the recoil proton will correspond to the elastic scattering of the incident electron with initial energy 6.6 GeV. There is complete overlap of the photon and proton arms. Both cover an almost full 2π azimuthal angle. The electron arm polar acceptance is $15.5 \pm 0.72^\circ$. The proton arm polar acceptance is $42.5 \pm 2^\circ$. If the electron beam energy is a bit less than 6.6 GeV, a slight shift of the electron arm acceptance will be done by moving the detector along the beam direction.

The solid angle of the electron detector for the selected momentum transfer range is 42 msr. The total cross section of elastic electron scattering in the detector acceptance is about 110 pb. At a projected luminosity of $1.6 \cdot 10^{38}$ cm^{-2}sec^{-1} the total rate of elastic events in the high resolution portion of the calorimeter is 15.6 kHz. Taking into account proton detector efficiency and a radiative tail of electrons, the rate of 14 kHz should be considered for statistics analysis. With 30 days of production running the estimated statistical error of the asymmetry result will be ± 5.2 ppm.

B. The systematics

The expected value of A_{PV} at $Q^2 = 2.5$ (GeV/c)^2 without SFF is 90 ppm. The projected statistical accuracy of the asymmetry value is 5 ppm, so the control of systematics on the level of 1 ppm will be sufficient. Coincidence between the proton and the electron may lead to a new possible systematics due to acceptance and efficiency correlations; however, it could be greatly reduced by using a proton detector of larger size and a collimator in front of the electron detector. This collimator is also useful for determination of the average value of momentum transfer. We are going to discuss systematics due to different backgrounds in the next sections.

- Beam polarization uncertainty.
- Helicity correlated beam position variation.
- Helicity correlated beam energy variation.
- Helicity correlated dead time of DAQ.
- Helicity correlated accidental events.

These systematics are common to the parity experiments, whose collaborations have developed a way to reduce systematics to a level below 0.1 ppm. The effect of the beam position variation to a large extent cancels out due to the 2π coverage of the electron detector, so even a huge 100 nm helicity related beam motion on the target is acceptable for this experiment. Energy variation with helicity flip due to beam intensity and orbit variation will be controlled by means already developed.

The raw counting rate of one DAQ subsystem in the proposed experiment is below 2 kHz. Systematics of the dead time correction was one of the serious problems of any counting method until the streaming readout was developed. The same problem is under investigation for SoLID in Hall A. The G0 experiment, which used the single arm counting method, has also solved the problem of dead time systematics.

C. Detectors single rates and accidentals

At a projected luminosity of $1.6 \cdot 10^{38}$ cm^{-2}sec^{-1} the singles rate on individual proton counters will be 4 kHz (threshold of 50 MeV) and the singles rate on the one electron counters will be 136 Hz (threshold 4.5 GeV). With 25 counters of the subsystem in the electron arm and 9 counters of the subsystem in the proton arm, such rates lead to an accidentals rate of 0.02 Hz for the 4 ns coincidence time interval. At the same time, real coincidences for such a subsystem will be 1.3 kHz. This allows already for a ratio of signal to accidental background of 6×10^4. Additional off-line cut on angular correlation provides another factor of 13. Off-line increase a cut on electron energy from 4.5 GeV to 5.1 GeV leads to another factor of 10. It is resulting in the Signal/Accidental ratio to be of 0.8×10^7.

D. Helicity in background processes

Accidental background may also have helicity asymmetry which will be taken into account by the usual method of extrapolation from the side time intervals.

We found that probability of background events in the collected event sample is relatively low mainly due to high energy precision on the electron arm energy and tight time and angular correlations between two particles in the event.

As was shown in section above the Real/Accidental ratio is the level of 0.8×10^7.

The beam polarization signal appears in the hyperon events, which value could be estimated from the cross section: 2% of the total inelastic $\gamma-$p cross section and hyperon decay: Taking into account the 30% polarization of the Λ and a 0.5 value of an asymmetry for Λ decay, the combined asymmetry is $1/(0.8 \times 10^7) \times 0.02 \times 0.15 =$ **0.4 ppb**.

Different type of accidental event is due to triple coincidence. Indeed, to get correct energy in the electron arm the electron arm could have two particles with strongly correlated energies. It requires a pseudo elastic event composed of two particles in one detector of the electron arm. One of those particle has low enough energy for inelastic event (hyperon production) and imitate an elastic event after a second particle hit the same electron detector. The rate of hits was estimated: inelastic process is of 110 kHz for 4.5 GeV threshold and triple for 3.8 GeV threshold. The probability to get second hit in electron arm counters could be estimated as $40 \times 10^{-9} \times 200 \times 10^3$, where the first factor is a time window; the second one is a hit rate with electron energy filling the gap to the elastic value. Resulting probability is of 1%, which is reduced then by the energy matching accuracy (2%) and by the fractional angular acceptance of the one electron arm detector: 3/1000. Relative rate of such triple hit events is of 0.6×10^{-6} or 0.06 Hz, which is 0.06 Hz/15 kHz = 4 ppm of the elastic event rate. Using a helicity correlated signal in the hyperon events, which value could be estimated from the cross section: 2% of the total inelastic $\gamma-$p cross section and hyperon decay main properties: the 30% polarization of the Λ and a 0.5 value of an asymmetry for Λ decay, the combined asymmetry is **0.01 ppm**.

Radiative processes associated with elastic electron scattering could also lead to the fifth structure function, as for example in Deeply Virtual Compton Scattering (DVCS). Logic of the triple hit again

could to be used to provide full energy in the electron arm detector but the resulting APV is low.

VI. EXPECTED RESULTS AND BEAM TIME REQUEST

A. Expected Results

The purpose of this experiment is to measure the A_{PV} with an accuracy sufficient to obtain conclusive evidence on SFFs at large momentum transfer. We will design and construct a full system with complete DAQ in about a year. In the production run the physics asymmetry A_{PV} will be measured to a statistical precision of ± 5.2 ppm. Table I presents a summary of the error contributions. The expected uncertainty of the G^s is $\pm 0.0025 \pm 0.0015$ or $\delta G^s / G_{Dipole} = \pm 0.05 \pm 0.03$, where the

#	quantity	absolute, ppm	relative
1	Count statistics	5.2	5.8%
2	Beam polarization	1.5	1.8%
3	ΔG_E^n	1.2	1%
4	Axial form factor	1.9	1.3%
	Total systematics		2.4%

TABLE I. The estimates of various contributions to the error of A_{PV} result.

first value is statistical error and the second value is systematical error.

B. Beam Time Request

The proposed experiment will be done at one beam energy of 6.6 GeV with currents up to 60 μA. A summary of the requested time is shown in Table II. For the production run we have the following periods: four shifts for commissioning of the polarized beam parameters and instrumentation, two shifts for calibration of the calorimeter with e−p elastic events and checkout of the boiling noise of the hydrogen target. We also request a total of three shifts during the running period to measure the beam polarization with the Moller polarimeter. The pion photoproduction background study will require a day of data taking with a 20 μA beam on the radiator in front of the hydrogen target (second loop). The total time requested is a sum of the concept test run, the required production beam time and the detector/beam calibration time. The total request for this proposal is 35 days.

Kin. #	Procedure	beam, μA	time days
C1	Beam parameters	1-70	1
C2	Detector calibration	10	2/3
C3	Dummy target data	20	1/3
C4	Beam polarimetery	1-5	2
C5	Pion yield study	20	1
E1	A_{PV} data taking	60	30
	Total requested time		35

TABLE II. The beam time request for the experiment.

VII. TECHNICAL CONSIDERATIONS

A. Time line of development

We expect that construction of the detector system will be done after completion of a set of approved NPS-based experiments in Hall C and the SBS program in Hall A which use HCAL.

B. The technology of calorimeters and DAQ

The technology and detectors themselves already exist, but the holding frames need to be designed. The current DAQ systems of both calorimeters are based on the flash ADC250 designed by JLab. They allow creation of a dead-time free readout system without significant new expenses. The plastic array will use a low-cost per channel TDC system .

C. The design considerations

The detector will be arranged in two parts, each of which will contain half of the proton and half of the electron ring calorimeters. These two sides moving horizontally to contact will provide the maximum solid angle possible for a given value of momentum transfer and its range. The positions of the detectors along the beam will be adjustable to take into account possible variation of the beam energy at the time of the experiment. The scattering chamber design will use a concept of the machined Al sphere proven in the E00-110 experiment. We may be can reuse parts of that scattering chamber.

D. Installation time

We expect that installation time (including the 10-cm-long LH2 cryotarget) will be within three months.

E. Collaboration

The Hall A/C collaboration consists of members with extensive experience with parity experiments in electron accelerators. In addition, the collaboration includes many individuals from the collaborations in Hall A/C with substantial experience in electromagnetic calorimetry and detectors for high energy hadrons.

VIII. CONCLUSION

We request 35 days of beam time for the measurement of the strange form factor of the proton at $Q^2 = 2.5$ (GeV/c)^2 in elastic scattering of 6.6 GeV electrons at 15.5°. This experiment will take place in Hall A, utilizing the polarized electron beam, a hadron calorimeter to detect protons, and an electromagnetic calorimeter to detect scattered electrons. This is the first experiment to measure A_{PV} in elastic electron scattering from the proton at Q^2 above 1 (GeV/c)^2. This experiment will be the first one to use coincidence between the electron and the recoiled proton to measure the PVA effect.

Knowledge of the strange form factor at large momentum transfer will allow determination of the size of the strange quark distribution function, which is crucial to the understanding of nucleon structure. We propose to measure A_{PV} to a statistical precision of ±5 ppm.

The projected statistical uncertainty of the form factor measurement is ±0.0025 (the G_D value is 0.049 at Q^2 =2.5 (GeV/c)^2). Such accuracy will allow significant improvement of flavor decomposition of the nucleon form factors, will test the lattice prediction, and may lead to observation of the non-zero SFF.

IX. PAC29 REPORT ON PR-06-004

There were several issues which PAC29 suggested evaluating (see its full text on the next page):

- "The PAC asked the proponents to consider performing the measurements at more than one Q2 value .." We agree that the measurement at 1 $(\mathrm{GeV}/c)^2$ will be very useful and close to G0 Q^2 range. It will require an additional 10 days of beam time.
- "... it may be more advantageous to restrict the measurements to Q2 values closer to the already existing data points." We do not expect sharp variation of the SFF, so the proposed scale between data points in Q^2 should be sufficient.
- "The PAC also asked the proponents to consider the necessary steps to exploit the flexibility of these non-magnetic detectors to possibly achieve a separation of the electric and magnetic SFFs." We made such analysis and found that the measurement at sufficiently low $\epsilon \sim 0.45$ will require significant additional beam time on the order of 100 days.
- "... the question of the dead time variation in coincidence mode remains open". Due to development of the flash ADC, the readout system currently could be arranged almost dead time free.
- "... the question of the effect of the rescattering of the outgoing polarized protons in the material between the target and the detector and inside the detector itself." We performed full MC simulation and found that the effect is sufficiently small, see Ref. [38].

Individual Proposal Report

Proposal: PR-06-004

Scientific Rating: N/A

Title: Strangeness form factor of the proton at 2 $(GeV/c)^2$

Spokesperson: B. Wojtsekhowski

Motivation: The proposal is aimed at measuring a combination of the strange form factors (SFF) at large Q^2, thereby extending the data at values larger than 1 $(GeV/c)^2$, which is the limit of experiments like G0 and HAPPEX. The ultimate goal would therefore be to verify if a large signal is observed for the SFF at such a high momentum transfer.

Measurement and Feasibility: This is a Parity Violation (PV) experiment where longitudinally polarized electrons (80%) scatter elastically on a proton target. The beam energy required is 6 GeV at a current of 100 μA. The principle (measuring PV asymmetries to access the weak form factors of the proton) is similar to other PV experiments performed at Jlab. However the experimental approach to access momentum transfers, Q^2, above 1 $(GeV/c)^2$ has to be rather different. It requires a coincidence experiment in a counting mode involving detection of both the scattered electron and the recoil proton in an electron and a hadron calorimeter. The calorimeters would cover 2π in azimuthal angle and would consequently be located at angles matching the kinematics of the elastic scattering process. The identification would be based on cuts on the kinematical correlations of the two particles and on the energy deposited in such non-magnetic counters. The experiment would require all the Hall A PV equipment that is necessary to keep experimental asymmetries at the level of a few ppm (the typical systematic limit for PV SFF experiments). In addition to that, the experiment would require building the two calorimeters, for which a concept has been developed and tested during a parasitic feasibility study. The proposal is asking for a 7 days beam time period for a concept test which will provide a 20% precision on the combination of the FF, and for a 33 days period for the measurement with the aim of reaching an error of about 0.1 on this combination. The feasibility does not appear guaranteed, in view of the various types of challenging backgrounds that may lead to helicity dependent effects, as outlined in more detail below.

Issues: The choice of the Q^2 value remains to be discussed in a general scheme of PV experiments at JLab (cf HappexIII vs G0). The PAC asked the proponents to consider performing the measurements at more than one Q^2 value and in particular suggested that it may be more advantageous to restrict the measurements to Q^2 values closer to the already existing data points. Given the exploratory nature of the first SFF measurement at higher Q^2, it would also make more sense to restrict such measurements to momentum transfer values where we can have a better understanding and interpretation of the SFF from a theoretical point of view. This is less obvious for measurements made at too high Q^2 values. The PAC also asked the proponents to consider the necessary steps to exploit the flexibility of these non-magnetic detectors to possibly achieve a separation of the electric and magnetic SFFs. From the technical point of view, while many concerns about control of beam parameters and other helicity dependent non-PV effects were carefully addressed in the proposal, the question of the dead time variation in coincidence mode remains open, as well as the question of the effect of the rescattering of the outgoing polarized protons in the material between the target and the detector and inside the detector itself. All these issues really demand a more thorough investigation and the PAC looks forward to seeing them addressed in a new proposal.

Recommendation: Defer

[1] T. Horn *et al.*, Scintillating crystals for the neutral particle spectrometer in hall c at jlab, Nuclear Instruments and Methods in Physics Research Section A: Accelerators, Spectrometers, Detectors and Associated Equipment **956**, 163375 (2020).

[2] G. Franklin, HCAL-J status (2014), report at SBS collaboration meeting, July, 2014.

[3] D. H. BECK and B. R. HOLSTEIN, Nucleon structure and parity-violating electron scattering, International Journal of Modern Physics E **10**, 1 (2001), https://doi.org/10.1142/S0218301301000381.

[4] F. Maas and K. Paschke, Strange nucleon form-factors, Progress in Particle and Nuclear Physics **95**, 209 (2017).

[5] D. B. Kaplan and M. Aneesh, Strange matrix elements in the proton from neutral-current experiments, Nuclear Physics B **310**, 527 (1988).

[6] R. D. McKeown, Sensitivity of polarized elastic electron-proton scattering to the anomalous baryon number magnetic moment, Physics Letters B **219**, 140 (1989).

[7] D. H. Beck, Strange-quark vector currents and parity-violating electron scattering from the nucleon and from nuclei, Phys. Rev. D **39**, 3248 (1989).

[8] P. A. Souder and other, Measurement of parity violation in the elastic scattering of polarized electrons from ^{12}C, Phys. Rev. Lett. **65**, 694 (1990).

[9] K. A. Aniol *et al.*, Measurement of the neutral weak form factors of the proton, Phys. Rev. Lett. **82**, 1096 (1999).

[10] D. S. Armstrong *et al.*, Strange-quark contributions to parity-violating asymmetries in the forward G0 electron-proton scattering experiment, Phys. Rev. Lett. **95**, 092001 (2005).

[11] F. E. Maas *et al.*, Measurement of the transverse beam spin asymmetry in elastic electron-proton scattering and the inelastic contribution to the imaginary part of the two-photon exchange amplitude, Phys. Rev. Lett. **94**, 082001 (2005).

[12] G. D. Cates, C. W. de Jager, S. Riordan, and B. Wojtsekhowski, Flavor decomposition of the elastic nucleon electromagnetic form factors, Phys. Rev. Lett. **106**, 252003 (2011).

[13] M. K. Jones *et al.* (Jefferson Lab Hall A), G(E(p)) / G(M(p)) ratio by polarization transfer in polarized e p —¿ e polarized p, Phys. Rev. Lett. **84**, 1398 (2000), arXiv:nucl-ex/9910005 [nucl-ex].

[14] M. Musolf, T. Donnelly, J. Dubach, S. Pollock, S. Kowalski, and E. Beise, Intermediate-energy semileptonic probes of the hadronic neutral current, Physics Reports **239**, 1 (1994).

[15] C. Prescott *et al.*, Further measurements of parity non-conservation in inelastic electron scattering, Physics Letters B **84**, 524 (1979).

[16] W. Heil *et al.*, Improved limits on the weak, neutral, hadronic axial vector coupling constants from quasielastic scattering of polarized electrons, Nuclear Physics B **327**, 1 (1989).

[17] B. Mueller *et al.* (SAMPLE Collaboration), Measurement of the proton's neutral weak magnetic form factor, Phys. Rev. Lett. **78**, 3824 (1997).

[18] D. T. Spayde *et al.*, Parity violation in elastic electron-proton scattering and the proton's strange magnetic form factor, Phys. Rev. Lett. **84**, 1106 (2000).

[19] K. A. Aniol *et al.*, Parity-violating electroweak asymmetry in e-p scattering, Phys. Rev. C **69**, 065501 (2004).

[20] A. Acha *et al.*, Precision measurements of the nucleon strange form factors at Q2 0.1 GeV2, Phys. Rev. Lett. **98**, 032301 (2007).

[21] Y. Zel'dovich, Electromagnetic interaction with parity violation, Sov. Phys. JETP **6**, 1184 (1958), Zhurnal Eksperimental'noi i Teoretischeskoi Fiziki, 33 (1957) 1531.

[22] S.-L. Zhu, S. J. Puglia, B. R. Holstein, and M. J. Ramsey-Musolf, Nucleon anapole moment and parity-violating ep scattering, Phys. Rev. D **62**, 033008 (2000).

[23] C. Chen, C. S. Fischer, C. D. Roberts, and J. Segovia, Form factors of the nucleon axial current, Physics Letters B **815**, 136150 (2021).

[24] C. Roberts, private communication (2022).

[25] Diehl, Markus and Kroll, Peter, Nucleon form factors, generalized parton distributions and quark angular momentum, Eur. Phys. J. C **73**, 2397 (2013).

[26] C. Alexandrou, S. Bacchio, M. Constantinou, P. Dimopoulos, J. Finkenrath, K. Hadjiyiannakou, K. Jansen, G. Koutsou, B. Kostrzewa, T. Leontiou, and C. Urbach (Extended Twisted Mass Collaboration), Nucleon axial and pseudoscalar form factors from lattice qcd at the physical point, Phys. Rev. D **103**, 034509 (2021).

[27] S. Riordan *et al.*, Measurements of the electric form factor of the neutron up to Q2=3.4 GeV2 using the reaction He-3$(e, e^{'} n)pp$, Phys. Rev. Lett. **105**, 262302 (2010).

[28] J. Xiangdong, Deeply virtual Compton scattering, Phys. Rev. D **55**, 7114 (1997).

[29] A. Radyushkin, Scaling limit of deeply virtual compton scattering, Physics Letters B **380**, 417 (1996).

[30] M. Guidal, M. V. Polyakov, A. V. Radyushkin, and M. Vanderhaeghen, Nucleon form factors from generalized parton distributions, Phys. Rev. D **72**, 054013 (2005).

[31] M. Goncharov *et al.*, Precise measurement of dimuon production cross sections in ν_μFe and $\overline{\nu}_\mu$Fe deep inelastic scattering at the fermilab tevatron, Phys. Rev. D **64**, 112006 (2001).

[32] T. J. Hobbs, M. Alberg, and G. A. Miller, Constraining nucleon strangeness, Phys. Rev. C **91**, 035205 (2015).

[33] T. J. Hobbs and G. A. Miller, private communication (2019).

[34] H. Mkrtchyan, private communication (2022).

[35] P. Degtiarenko, private communication (2022).

[36] B. Reydo, Trigger with fADC-based systems (2022).

[37] Y. Roblin and F. Sabatie, DVCS experiment E00-110 (2000).
[38] A. Blitstein and B. Wojtsekhowski, Simulation of the spatial shift in detector response for polarized protons within a calorimeter, Nuclear Instruments and Methods in Physics Research Section A **1031**, 166565 (2022).